Hydrogeophysical characterization in a volcanic context from local to regional scales combining airborne electromagnetism and magnetism

Marc Dumont[1], Pierre-Alexandre Reninger[2], Bertrand Aunay[2], Alexandre Pryet[3], Damien Jougnot[1], Jean-Lambert Join[4], Laurent Michon[5], and Guillaume MARTELET[6]

[1]Sorbonne Université
[2]BRGM
[3]Institut Polytechnique de Bordeaux
[4]University of La Réunion
[5]Université de la Réunion, Institut de Physique du Globe de Paris
[6]Bureau de Recherches Geologiques et Minieres

November 30, 2022

Abstract

In volcanic islands, a crucial step for watershed resources management is the characterization of groundwater aquifers from local to regional scales. Airborne geophysical data provide high-resolution imagery down to hundred meters below the surface, over large territories. Yet, its regional accurate interpretation may be limited by the low density of field observations. In this study, we propose an approach combining airborne electromagnetic and magnetic data in order to resolve ambiguities and provide a multiscale hydrogeophysical characterization of Piton des Neiges volcano (Réunion Island). With limited calibration data, this methodology produces a geological model more robust and accurate than using airborne electromagnetic data alone. Through the continuous coverage of both methods, we demonstrate the influence of volcanic unit geometries on groundwater flows within the critical zone and we highlight major structures impacting groundwater flows at both local and regional scales.

Hosted file

`grl_supportinginformation.docx` available at https://authorea.com/users/71035/articles/607682-hydrogeophysical-characterization-in-a-volcanic-context-from-local-to-regional-scales-combining-airborne-electromagnetism-and-magnetism

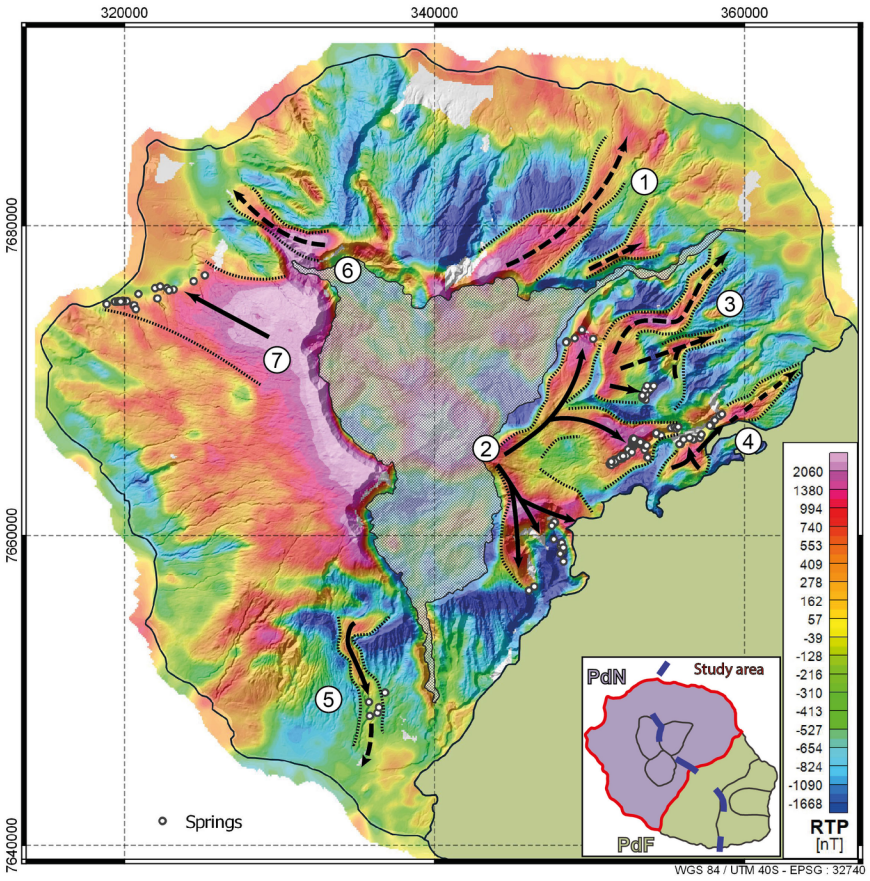

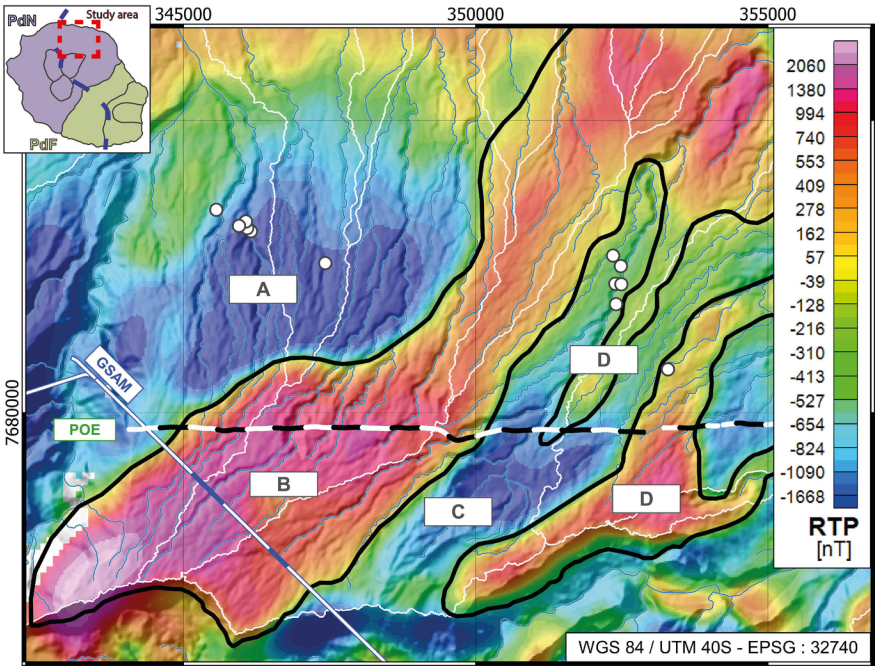

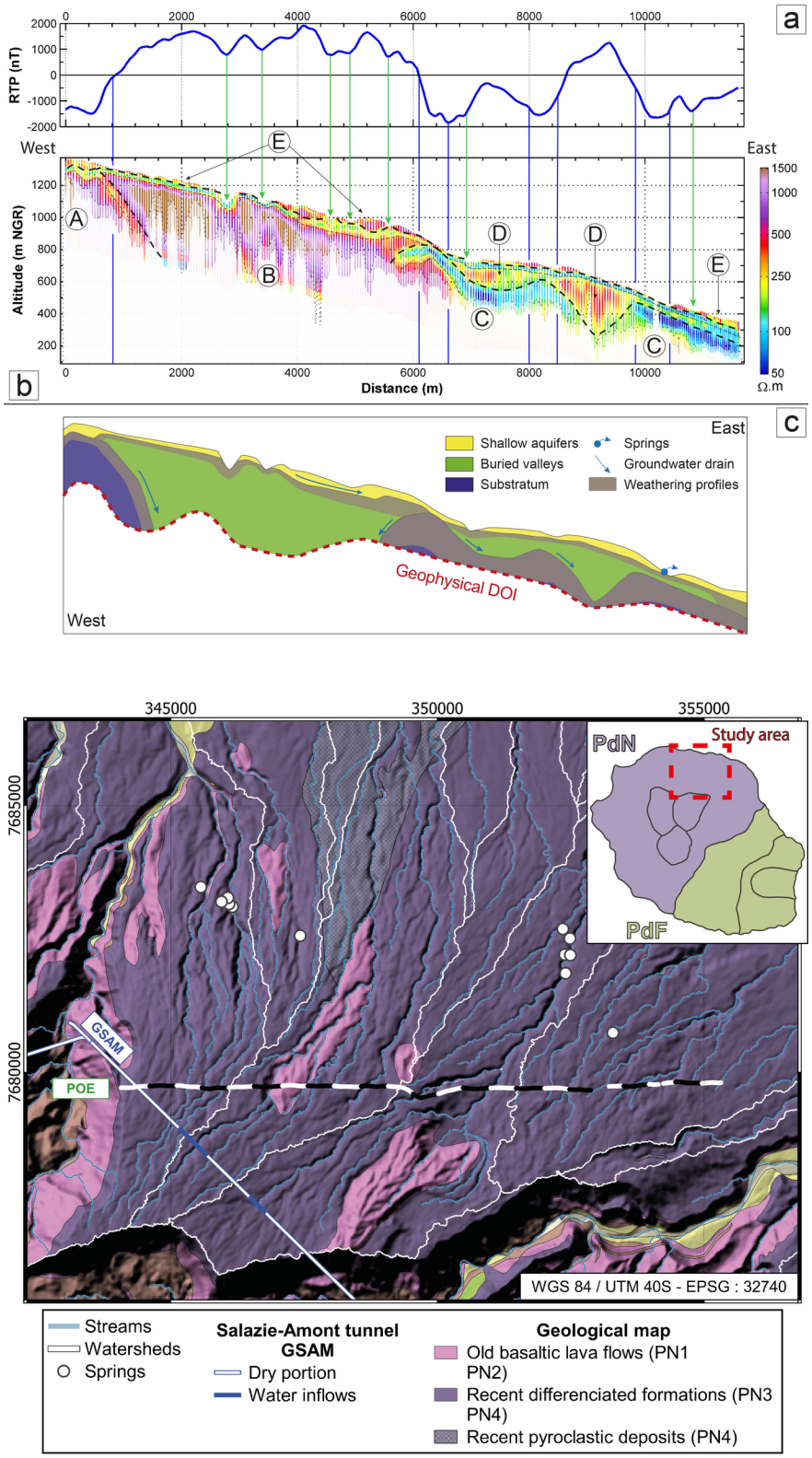

Hydrogeophysical characterization in a volcanic context from local to regional scales combining airborne electromagnetism and magnetism

M. Dumont[1,2,3,4], P.A. Reninger[5], B. Aunay[3], A. Pryet[6], D. Jougnot[3], J.L. Join[1,2], L. Michon[1,2], and G. Martelet[4]

[1] Université de La Réunion, Laboratoire GéoSciences Réunion, F-97744 Saint-Denis, France

[2] Université de Paris, Institut de physique du globe de Paris, CNRS, UMR 7154, F-75005 Paris, France

[3] BRGM, Reunion Island Regional Office, F-97400 Saint-Denis, France.

[4] Sorbonne Université, CNRS, EPHE, UMR 7619 METIS, 75005 Paris, France.

[5] BRGM, UMR 7327, BP 36009, F-45060 Orléans, France.

[6] EA 4592 Géoressources et Environnement, Bordeaux INP and Université Bordeaux Montaigne, Pessac, France.

Corresponding author: Marc Dumont (dumont.mrc@gmail.com)

Key Points:

- Magnetic measurements help constrain the hydrological interpretation of resistivity models in volcanic settings.
- Hydrogeophysical interpretations of deep airborne electromagnetic imagery unveil groundwater stratified flows between volcanic units.
- Coupled analysis of airborne electromagnetic and magnetic dataset allows us to improve groundwater management from local to regional scale.

Abstract

In volcanic islands, a crucial step for watershed resources management is the characterization of groundwater aquifers from local to regional scales. Airborne geophysical data provide high-resolution imagery down to hundred meters below the surface, over large territories. Yet, its regional accurate interpretation may be limited by the low density of field observations. In this study, we propose an approach combining airborne electromagnetic and magnetic data in order to resolve ambiguities and provide a multiscale hydrogeophysical characterization of Piton des Neiges volcano (Réunion Island). With limited calibration data, this methodology produces a geological model more robust and accurate than using airborne electromagnetic data alone. Through the continuous coverage of both methods, we demonstrate the influence of volcanic unit geometries on groundwater flows within the critical zone and we highlight major structures impacting groundwater flows at both local and regional scales.

Plain Language Summary

Groundwater characterization from local to regional scale is an essential element especially for sustainable water policy. In volcanic setting, the complexity of the subsurface and geological structures are still poorly integrated into hydrological models leading to uncertainties on predicting models. Our study aims to combine two geophysical methods acquired during airborne surveys over Réunion Island in order to improve the accuracy of airborne geophysical interpretation without limited external information, characterize structures and their influences on groundwater flows, and upscale these results from local to regional scales. The methodology may be applied to other complex geological settings in order to integrate local and regional heterogeneities into hydrological models.

1 Introduction

In volcanic islands, understanding the distribution of groundwater reservoirs, their dynamics and connection at the island scale is critical for drinking water autonomy. For decades, two hydrogeological conceptual models associated with the Canary and Hawaiian Islands have characterized different hydrogeological functioning between the coastal and the inland areas (Custodio et al., 1988; Peterson, 1972). While groundwater aquifers are clearly identified and reachable in coastal areas (Gingerich & Voss, 2005; Herrera & Custodio, 2014), the thickness of lava flows' unsaturated pile can reach up to thousands of meters in volcanos' central parts. This results in a thick vadose zone where groundwater flows follow complex geological structures due to a polygenetic volcanic activity (Izquierdo, 2014; Vittecoq et al., 2014), and because of the evolution of hydrodynamic properties of volcanic rocks due to weathering and alteration processes (Custodio, 2004; Join et al., 2005; Lachassagne et al., 2014). The groundwater is thus classified in three different aquifer categories based on the above-mentioned geological parameters: shallow aquifers, perched aquifers and basal aquifers (Join et al., 2016). Due to the thickness of the vadose zone, inland aquifer geometries remain unclear. Nevertheless, as they benefit from the highest recharge rates, inland aquifers drain significant groundwater to coastal basal aquifers, which are vulnerable to saltwater intrusion (Oki et al., 1998; Pryet et al., 2012). Thus, it is critical to estimate inland aquifers location, geometries, and extension in order to understand their possible impact on basal aquifers' recharge rates. To this end, the vadose zone needs to be studied on both local and regional scales to define aquifers' geometries and groundwater watersheds (Vittecoq et al., 2019).

Over the last decades, near-surface geophysics applied to environmental issues have paved new ways to characterize geological and hydrological contrasts from local to regional scales (Binley et al., 2015; Parsekian et al., 2015). One of the main objectives of hydrogeophysics is to provide reliable and meaningful images of the subsurface with the best spatial resolution. However, since it is essential to integrate local heterogeneities into larger groundwater behaviors, mapping groundwater pathways at a watershed level and on a regional scale remains challenging. In order to address this issue, we use airborne time domain electromagnetic (TDEM) and total magnetic field (Sørensen & Auken, 2004) data to image the subsurface's electrical resistivity and magnetic properties at a regional scale, along up to several thousands of kilometers of flight lines (Chandra et al., 2019; Ley-Cooper et al., 2019). As it is sensitive to lithological contrasts, clay content, groundwater saturation, and salinity, airborne electromagnetic (AEM) is an efficient method to tackle several groundwater issues (Ball et al., 2020; Foged et al., 2014; Minsley et al., 2012; A. Viezzoli et al., 2012). Nevertheless, this method encounters significant limitations, especially in complex settings, because of resistivity model ambiguous meaning. Collected data need to be compared with other ones, such as geological, geophysical and/or groundwater measurements.

Here, we use a methodology combining both AEM and magnetic data to (i) unravel resistivity ambiguity issues and achieve a geological model of the critical zone in volcanic settings, and (ii) improve our understanding of large-scale groundwater flows within the vadose zone. In order to obtain a consistent methodology across scales, our approach is focused on the optimal use of airborne geophysical dataset to tackle multiscale issues using petrophysical benchmark, and results from previous studies. The objective is to define the most robust and precise geological structures across scales, incorporating uncertainties that only local multidisciplinary studies can resolve.

Applied to Réunion Island (Indian Ocean), composed of two basaltic volcanoes, this approach has been used to characterize the stratification of groundwater flows within the north-eastern slope of Piton des Neiges volcano. The resistivity model informs us on both lithological and permeability contrasts below the surface, down to 500 m. Magnetic measurements provide integrated information on geological structures and can differentiate lava flows, especially if the stratigraphy contains normal and reversely magnetized flows (Gailler & Lénat, 2012). AEM provides an accurate 3D imagery of lithological units, while the extension of volcanic units is defined with magnetic maps. The combined analysis of both geophysical imageries mitigates resistivity and magnetic interpretation limits in complex geological contexts. As local studies unravel buried valleys magnetic patterns, they can be upscaled to delineate major hydrogeological structures over the entire Piton des Neiges volcano, highlighting the presence of large-scale volcanic structures.

2 Study area and Methods

Réunion Island, is a volcanic island located in the western part of the Indian Ocean (Figure 1). Our study focuses on Piton des Neiges volcano resulting from the accumulation of basaltic and trachybasaltic flows (Salvany et al., 2012), during the last two magnetic periods — the reversed Matuyama (2.581-0.78 Myrs) and normal Brunhes (0.78-0 Myrs; Lénat et al., 2001). The emerging volcanic period, called La Montagne (LM), occurred between 3 Ma and 1.8 Ma producing basaltic rocks.

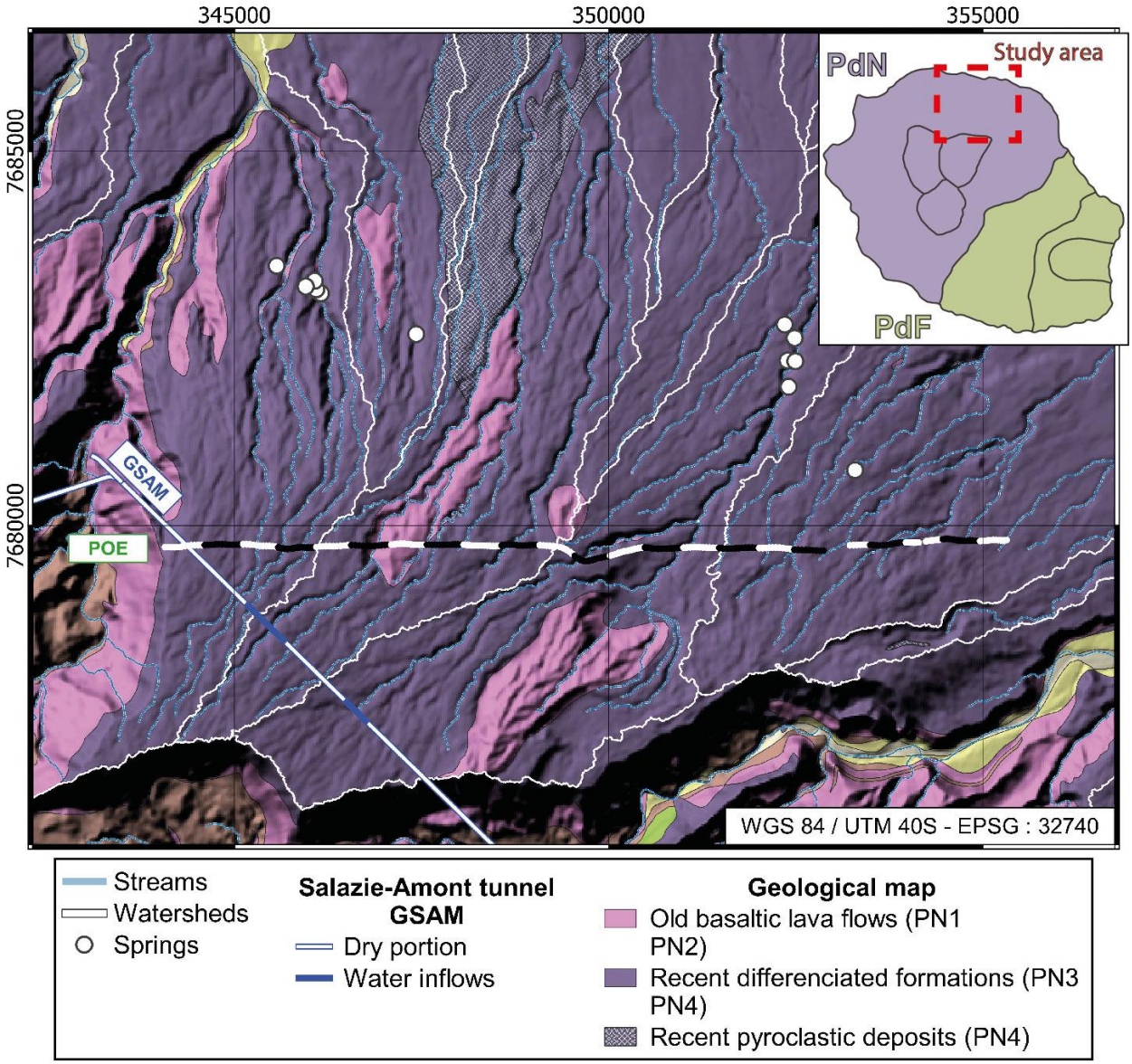

Figure 1. Geological map of Plaine des Fougères, part of the northern flank of Piton des Neiges (modified from Billard, 1974). The inset represents Réunion Island with Piton des Neiges (PdN) and Piton de la Fournaise (PdF) volcanoes. POE line locates the AEM profile shown in Figure 2.

The two subsequent eruptive periods, PN1 (1.4-0.95 Ma) and PN2 (0.6-0.43 Ma), built successive edifices made of basaltic lava flows. After a lull of 90 kyrs, differentiated magmas led to the construction of PN3 (340-180 ka) and PN4 (140-29 ka; Salvany et al., 2012). The five eruptive periods were separated by lulls characterized by both weathering and destructive processes (Gayer et al., 2019). At Réunion Island, magnetic anomalies are mainly controlled by thermoremanent magnetization (Gailler & Lénat, 2012). Basaltic rocks are characterized by a high magnetic intensity, and a magnetic polarity and orientation inherited from the geomagnetic field at their age of emergence (average Koenigsberger ratio is above 7 - Chauvin et al., 1991). These characteristics do not vary with time and weathering processes induce a slight intensity

decrease. Thus, inverse magnetization refers to LM and PN1 formations, whereas normal ones relates to PN2 to PN4 units.

The volcano's history, including alternating constructive and destructive periods, results in a complex imbricated structure (Salvany et al., 2012). To understand how the different volcanic units (i.e. lava flows from the same eruptive period) are structured according to the volcano's history, we first focus on the north-eastern slope of the volcano, Plaine des Fougères (90 km^2), extending from 200 to 1,800 m above sea level (Figure 1). The substratum of the area includes the oldest LM and PN1 formations with outcrops in the southern part of the area and in steep ravines. Outcrops of these formations are also visible in a deeply drilled tunnel called Salazie-amont (GSAM), which crosscuts the study area 1,000 m below the surface and intersects three aquifer sectors (Figure 1; Maréchal et al., 2014). The planeze consists of homogeneous pyroclastic units emplaced during PN3 and PN4 overlapping differentiated PN3 lava flows. The study area, located more than 10 km away from the volcano's center, is too distant to be influenced by active hydrothermal processes (Bénard et al., 2019).

A SkyTEM survey was conducted over the entire island (more than 2,500 km^2; Figure 1; Martelet et al., 2014). Airborne electromagnetic data were acquired ~30 m along flight lines with a low moment to ensure near-surface resolution and a high moment to increase the depth of investigation (Sørensen and Auken, 2004). During the high moment off-times, the magnetic field was measured providing the same lateral resolution. On the regional scale, the electromagnetic dataset was processed with a standard processing scheme developed by HGG© (Auken et al., 2009). Over the Plaine des Fougères area, a specific scheme was applied to improve AEM data density and resolution (Reninger et al., 2019). Both AEM inversions were achieved using quasi-3D spatially constrained algorithm (Viezzoli et al., 2008). AEM inverted smooth models discretizes the subsurface in 25-30 layers (regional-local models characteristics). The layer thickness increases logarithmically with depth from 5-2 m thick for the first one up to a depth of 350-500 m. Magnetic data were processed according to the industry standards, with diurnal removals and IGRF (International Geomagnetic Reference Field) correction, resulting in a Residual Magnetic Field. Reduction to pole (RTP) was then performed to move anomalies over their sources and the X-Y shift of magnetic anomalies created by the geomagnetic field's inclination (Baranov, 1957). However, no corrections have been applied to decrease topographic impact on magnetic measurements. Magnetic maps were produced using Geosoft software.

Prior to interpreting geophysical imagery results, we develop here several theoretical concepts and paradigm important for our approach. First, all volcanic products resulting from the same eruptive period form a volcanic unit comprising a stack of lava flows and pyroclastic interflows. Between two eruptive periods, superficial formations are exposed to weathering and erosion processes, which creates weathering profiles at the top of every volcanic unit (Gayer et al., 2019). These weathering profiles could consist of either weathered allochtone or eroded volcanic rocks, or a combination of the two. As a result, the volcanic heterogeneity and the impact of weathering processes lead to resistivity contrasts within each volcanic unit. Thus, in order to take such complexity into account, geo-electrical features should be defined based on geometries instead of resistivity values. Each feature could thus be composed by resistive and conductive layers. Second, as groundwater circulates through these formations, resistivity will be impacted by two parameters: saturation and clay content. In order to understand the influence of each parameter, a benchmarking is developed in supplementary materials S.1. Using Waxman & Smits petrophysical model (1968) with basaltic volcanoes characteristics, we show that

resistivity can vary by one order of magnitude because of the water saturation whereas it ranges by three orders of magnitude due to clay content. Considering that pyroclastic interflows account for lower volumes than basaltic lava flows (Custodio, 2004), and that AEM integrates high ground volumes, clay content has more influence on resistivity variations than water saturation.

3 Multi-method airborne geophysical interpretations

In order to present our interpretation, we present the 2D resistivity section named POE (Figure 2b), where all geo-electrical features observed on the slope — labeled A to E — are imaged. Nevertheless, the same analysis was carried out on 35 profiles (along 275 km of flight lines) validating the five geo-electrical features consistency and extension, and related magnetic variations (four different 2D resistivity profiles are presented in supplementary S.2.). On profile POE, a thin resistive layer (≈500-800 Ω·m) mantle the surface (E). Below, features A and C consist of a 50 to 200 m thick conductive layer (<100 Ω·m) overlaying a resistive body (>1,000 Ω·m). For both features, the resistive and conductive layers show the same geometry with a wide base at depth and oblique vertical limits. B feature corresponds to a large resistant body (800-1,500 Ω·m) in the center of the profile whose oblique limits converge in depth. D feature contains of U-shaped resistive layers (500-1,000 Ω·m) covered by thin conductive horizon (≈100-200 Ω·m). Each of the 5 features is therefore characterized by a resistant horizon surmounted by a more or less important conductive layer. Their spatial coherence as well as their geometries are consistent with superimposed units of different eruptive periods. Feature A and C should correspond to old altered lithologies and features B and D are lithologies covering old formations. Finally, feature E corresponds to recent volcanic formation structure. However, the low AEM near-surface resolution does not allow us to define whether a weathering profile has been developed in this superficial horizon.

The age of the imaged lithological units is determined from their magnetic signatures, using magnetic polarity variation from one volcanic unit to another. POE profile can be divided into three major parts: two magnetic lows at the edge of the profile corresponding to old LM and PN1 units, and a magnetic high in the center related to young formation PN2 to PN4. The lateral extension of these structures is consistent with geo-electrical feature extensions (Figure 2a). On a smaller scale, the magnetic anomaly amplitude increases where feature D thickens, and decreases where E is eroded (see green arrows in Figure 2a). Features A and C are associated with magnetic low (≈-1,500 nT) corresponding to old volcanic units (LM and/or PN1). In both cases, the magnetic response is substantially identical, while feature A is characterized by a thin weathered horizon and C is mainly composed of thicker conductive layer reflecting higher weathering rates. This demonstrates the predominance of polarity inversion on magnetic intensity decrease produced by volcanic rocks weathering. Filling the old morphology, features B and D reflect two major buried paleo-valleys filled with younger magnetic lavas, likely PN2 and PN3, reflected by magnetic highs. During these two phases, the volcano was active with a short period of inactivity that did not allow the establishment of a significant alteration profile. The AEM resolution does not allow to image the limits between PN2 and PN3 units. The shallow part of the slope mainly consists of a thin resistive layer (E), which increases locally the major magnetic anomaly created by B feature (with a maximum intensity of approximately 1,000nT where the layer is the thickest). Its geophysical characteristics and its geometry are consistent with outcropping PN4 formations that appear clearly at the outcrop (Figure 1).

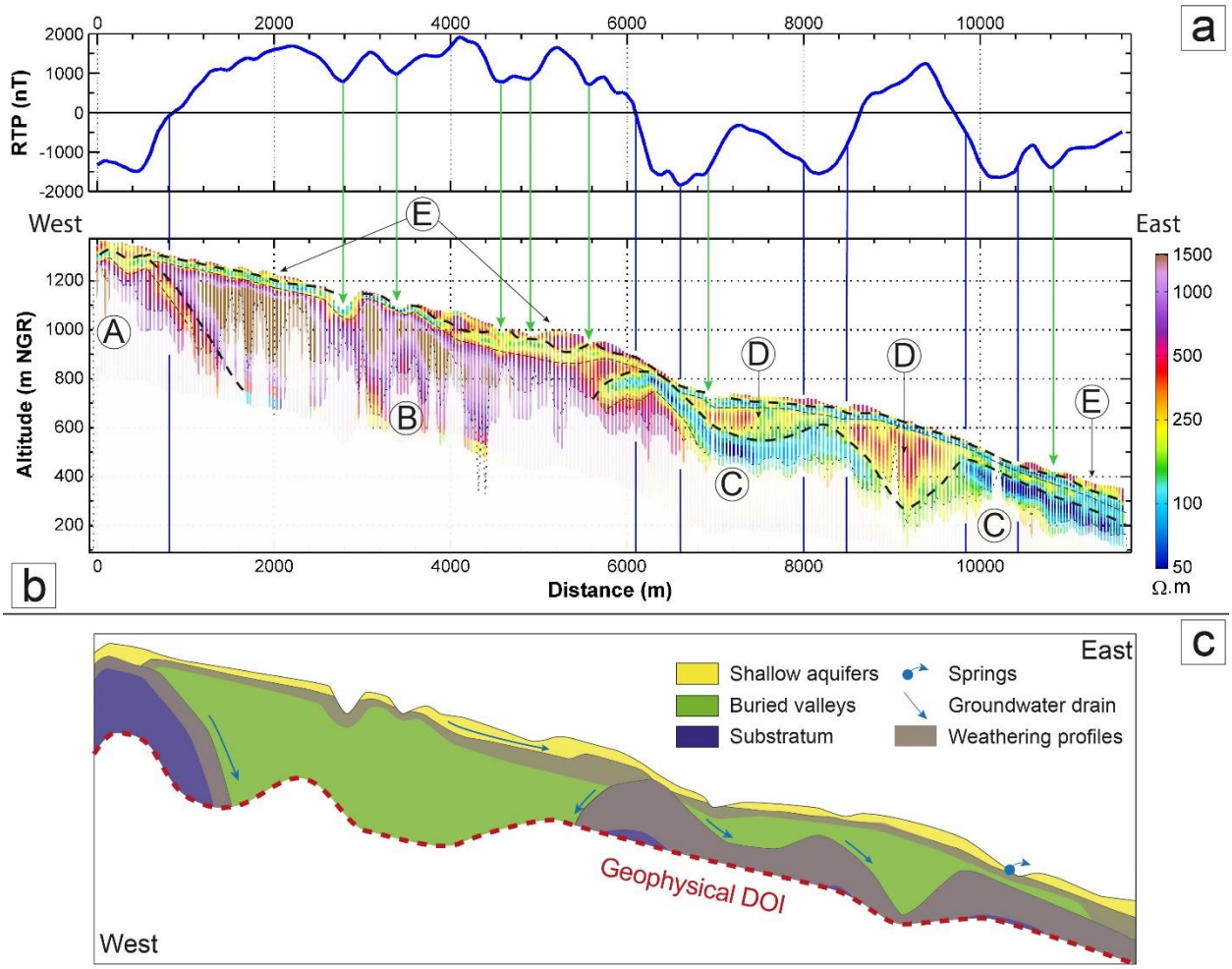

Figure 2. POE (**a**), reduced to the pole magnetic signal (**b**), and resistivity profiles, crossing the Plaine des Fougères area from west to east. Five features (A to E) are identified in the resistivity profile, separated by black dashed lines. Blue lines highlight magnetic anomaly limits. Green arrows show locations where RTP signal is affected by the lack of PN4 formations, in ravines. (**c**) Conceptual groundwater model based on hydrogeophysical interpretations. Shallow aquifers result from later volcanic products from pyroclastic units of the end of PN3 and PN4 eruptive periods. Buried valleys are filled with PN2 and PN3 lava flows. The substratum is characterized by old weathered lava flows from LM and/or PN1 eruptive periods.

The following step consists in comparing the main structures based on airborne data and hydrogeological data in order to understand water flow behaviors within the critical zone. Previous studies analysed several springs at the bottom of Plaine des Fougères volcano slope demonstrating the presence of limited shallow aquifers, emerging at the limit between recent formations overlaying older ones (Aunay et al., 2012). According to airborne data, the superficial thin resistive layer (feature E) overlays weathered older formations. In supplementary materials, S.2.d and S.2.e profiles demonstrate that springs are located where erosive structures intersect the limit between PN4 formations and older ones. In these cases, the aquifer is present in unaltered shallow formations inducing only a slight decrease in resistivity (see supplementary material S.1.). In contrast, the aquifer lies beneath paleo-profiles of older formations where the increase in clay content, as well as the saturation of these impermeable formations, significantly

decreases the resistivity. Nevertheless, the resolution of airborne geophysics does not allow to precisely define the boundary between saturated and weathered horizons. It is reasonable to consider that groundwater flows occur at the bottom of resistive features as at the top of conductive ones. This demonstrates the impact of volcanic units limits, which create lateral pathways at the limit between young formations overlaying old weathered ones. Thus, springs could emerge when these geological boundaries are intersected by the hydrologic network in the slope/flow direction. These results may suggest that paleo-weathering profiles drain groundwater flows, creating aquifers at the bottom of volcanic units (Figure 2c).

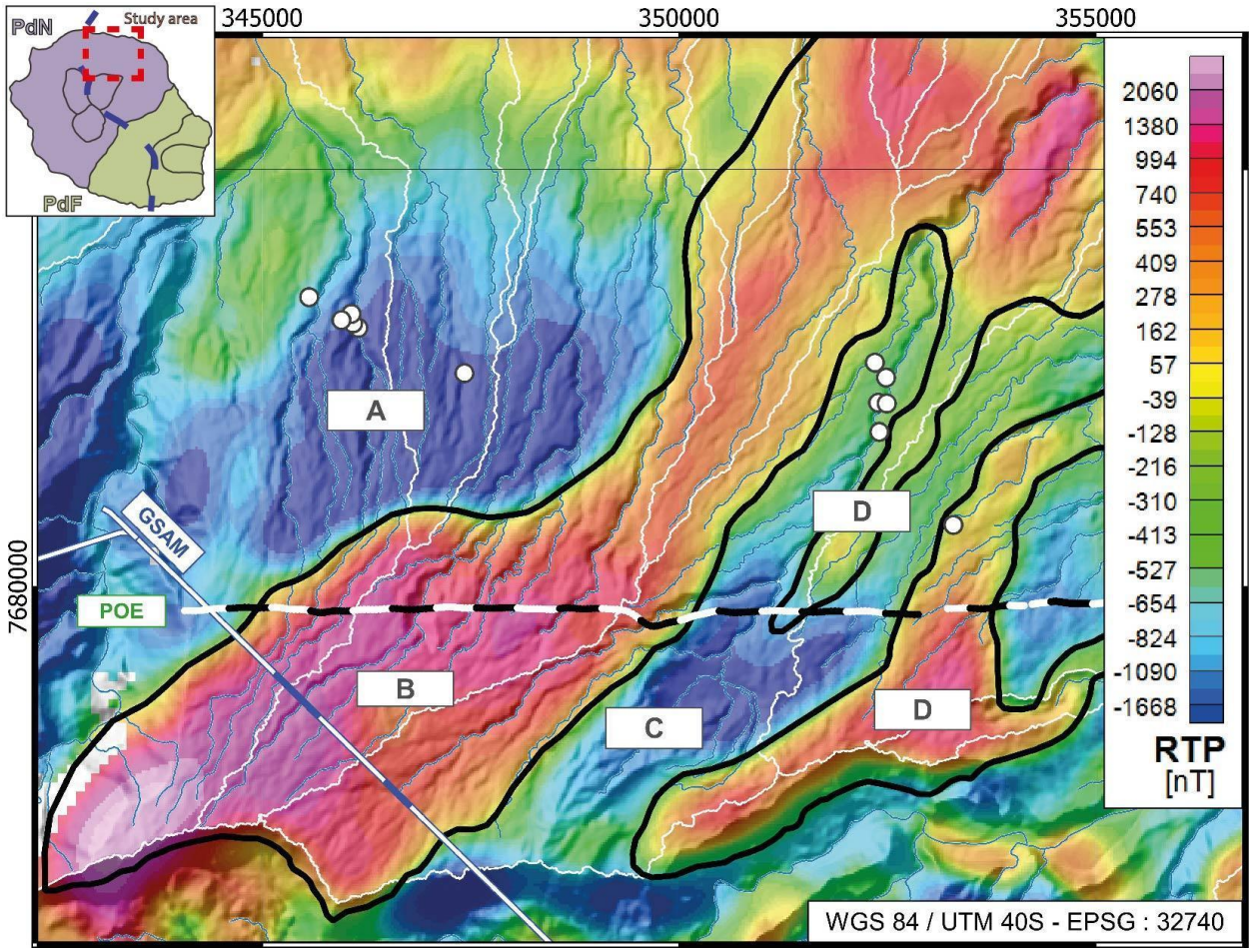

Figure 3. Mapping of two large paleo-valleys eroded between PN1 and PN2 periods using magnetic map (reduced to the pole). 2D POE profile is indicated in black and white, changing colors every 500 m to ease the comparison with Figure 2. Deeply drilled tunnel GSAM is indicated in white, with blue parts corresponding to groundwater outflows. Watersheds of the slope are represented with white lines. The inset represents Réunion Island with both volcanoes — Piton des Neiges (PdN) and Piton de la Fournaise (PdF).

Previous hydrogeological studies in the deep tunnel demonstrated that water inflows are observed where the tunnel goes through PN2/3 recent formations, below magnetic feature B (Figure 3). An analytical solution have been used to model groundwater inflows within the tunnel during the drilling (Maréchal et al. 2014). Model calibrated permeability of old LM/PN1 formations ranges from 10^{-7} to 10^{-9} m/s, while PN2/PN3 permeability are between 10^{-4}-10^{-6} m/s.

This could induced groundwater drainage at the interface between the substratum and the paleo-valley (Figure 2c). This result would reveal that feature B, the main imaged paleo-valley, is 1,000 m thick and drains large volumes of groundwater, as demonstrated by water inflows into the tunnel (up to 2,000 L/s; Maréchal et al. 2014).

The results obtained in Plaine des Fougères are summarized in a conceptual groundwater model presented in Figure 2c. The volcano's slope includes three major structures considered as reservoirs with less permeable weathering profiles at the top. The semi-permeable substratum comprises old weathered formations from LM and/or PN1 volcanic periods. Because of a long quiescence period between PN1 and PN2 periods, the substratum has been eroded, creating two large valleys. When the volcano activity restarted, both filled up with PN2 and PN3 products, and since then, they have drained groundwater through Plaine des Fougères slope. The shallow part has been shaped by the most recent formations from PN4, supporting the emergence of limited aquifers. However, because of geophysical limitations and poor geological information, the volcanic units within the substratum and the buried valleys cannot be precisely described. This geological structure induces stratified groundwater circulations within the critical zone of Plaine des Fougères slope. The presence of three volcanic units creates groundwater stratification and significant drainage within both paleo-valleys. Based on geophysical results, such stratified groundwater circulations should occur in the fresh volcanic formations supported by the weathered aquitards from the older volcanic units, which could be saturated at the top. Nevertheless, AEM resolution cannot allow to define this precisely.

4 Local to regional upscaling approach

The local study has brought to light the presence of major buried valleys draining groundwater from rainy peaks to the coast. Such structures are well-known for impacting groundwater circulation (Charlier et al., 2011; Lachassagne et al., 2014). In supplementary material S.3., we first analyzed the ability of resistivity model to image the extension of such structures. Nevertheless, their limits and extensions remain unclear and cannot be mapped with simple depth/altitude resistivity slices. This is why we explored the potential of magnetic mapping. On the RTP map (Figure 3), the two major buried valleys of Plaine des Fougères are clearly delineated by positive anomalies (1; Figure 4). In line with 3D resistivity contrasts, both paleo-valleys cross the entire slope from the top to the coastal area (south-west to north-east). This radial orientation is specific to erosive structures, which emphasizes our interpretation about filled, buried valleys (Macdonald et al., 1983). Furthermore, similar patterns displayed on the RTP map (i.e. a positive anomaly oriented from the center to the external part of the volcano) may indicate the presence of buried valleys filled with PN2, PN3 and/or PN4 products.

At local scale, this study has brought to light large buried valleys, without any topographic clues. Thanks to our combined approach, seven structures have been identified at regional scale. Most of them support groundwater flows emphasized by springs or highly productive aquifers partially known by local operators. All these elements have unveiled hidden major buried valleys, which drain groundwater flows through several hydrological watersheds (Figure 3). As described by previous studies (Charlier et al. 2011; Vittecoq et al. 2014, 2019), this certainly affects water balance estimation due to a concentration of groundwater resources at the bottom of buried valleys. A combined interpretation of electromagnetic and magnetic datasets makes it possible to delineate them in order to (i) implement groundwater watersheds in

regional water balance estimation, and (ii) identify areas of interest for future groundwater studies.

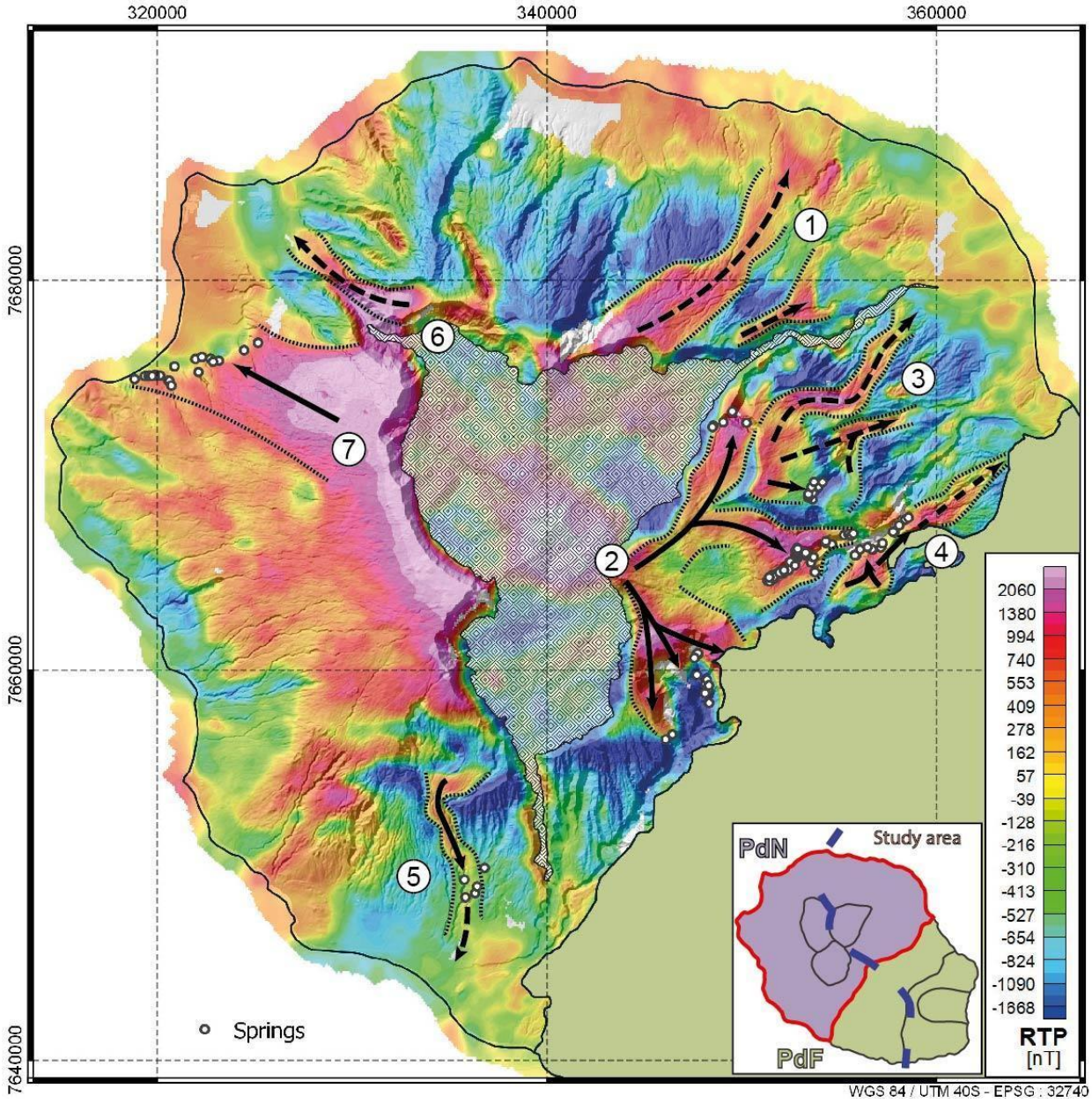

Figure 4. Magnetic signatures interpreted as buried valley patterns are delineated and numbered on the RTP map throughout the Piton des Neiges area. Seven hydro-geological structures are delineated by dashed lines: (1) Plaine des Fougères, (2) Bébour and Bélouve, (3) Massif de l'Est, (4) Ilet Patience and Massif cratère, (5) Les Makes, (6) St-Paul, and (7) Dos d'âne. Groundwater flow pathways appear as black arrows varying according to superficial evidence: (i) solid arrows when groundwater is drained to superficial springs, and (ii) dashed arrows where there is no superficial evidence. The inset represents La Réunion Island with both volcanoes — Piton des Neiges (PdN) and Piton de la Fournaise (PdF).

5 Conclusions

In this study, we present a multi-scale approach combining electromagnetic and magnetic data from airborne survey in order to understand groundwater pathways through the critical zone. From the results of previous studies on volcanic context hydrology and geology, as well as petrophysical benchmark, factors influencing both geophysical signals have been identified. Based on this, the combination of electromagnetic and magnetic data allowed to reduce the uncertainty of hydrogeophysical interpretations. While resistivity imaging enables the determination of clay content variations, the use of magnetic measurement allows the identification of geological structures in the critical zone.

We were able to define a conceptual geological model delineating major structures of the main study area. We have shown that, contrarily to the general hydrological paradigm, old and slightly altered formations can be present in depth. When compared to a limited number of groundwater field data, it is possible to highlight a link between weathering paleo-profiles and groundwater pathways organization within the deep critical zone of shield volcanoes, which is rarely studied. Using volcanic units as representative elementary volume, our approach does not allow a detailed analysis of all the processes involved. Instead, the simplification of the groundwater behaviors allows to extrapolate these results at regional scale. The presence, extension and orientation of seven major structures were thus defined. Some known and previously studied structures allowed to improve the validation of the conceptual model, while new unknown structures were revealed.

This hydrogeophysical study tackling both geophysical and groundwater issues open up several perspectives. Demonstrating the interest of the combined interpretation of airborne electromagnetic and magnetic dataset, we support the opinion that joint inversion of both methods, rarely performed, would allow the construction of robust and accurate models reducing geophysical uncertainties. From a groundwater resource perspective, our study highlights the importance of deep circulations controlled by volcanic structures. Hence, the integration of such structures at the watershed scale will allow to better estimate the recharge of coastal aquifers, the main resources in an insular volcanic context, and to define potential targets for water supply of inland populations.

Acknowledgments, Samples, and Data

This work as well as the SkyTEM survey in Réunion Island were supported by La Réunion local government, the European Union (through FEDER funding), the Office de l’Eau de La Réunion (Réunion Water Commission) and the BRGM. Airborne electromagnetic and magnetic data for thisresearch are not publicly available due to diffusion restriction from the survey founders. Data are presented in this citation references: Marteletet al., 2014; Reninger et al., 2019, and could be acquired under a free licensing. Please contact the authors of previous citations to establish a license and obtain the data. Datasets for the petrophysical analysis are included in this paper: Archie, 1942; Custodio,2004; Join et al., 1997; Soueid Ahmed et al., 2018; Woudruff and Revil, 2011.

References

Auken, E., Christiansen, A. V., Westergaard, J. H., Kirkegaard, C., Foged, N., & Viezzoli, A. (2009). An integrated processing scheme for high-resolution airborne electromagnetic surveys, the SkyTEM system. *Exploration Geophysics, 40*(2), 184–192. https://doi.org/10.1071/EG08128

Ball, L. B., Bedrosian, P. A., & Minsley, B. J. (2020). High-resolution mapping of the freshwater–brine interface using deterministic and Bayesian inversion of airborne electromagnetic data at Paradox Valley, USA. *Hydrogeology Journal, 28*(3), 941–954. https://doi.org/10.1007/s10040-019-02102-z

Baranov, V. (1957). A new method for interpretation of aeromagnetic maps: Pseudo-gravimetric anomalies. *GEOPHYSICS, 22*(2), 359–382. https://doi.org/10.1190/1.1438369

Billard, G. (1974). *Carte Géologique de la France, La Réunion. Quatre feuilles + notice 40 p.* (BRGM) [Map].

Binley, A., Hubbard, S. S., Huisman, J. A., Revil, A., Robinson, D. A., Singha, K., & Slater, L. D. (2015). The emergence of hydrogeophysics for improved understanding of subsurface processes over multiple scales. *Water Resources Research, 51*(6), 3837–3866. https://doi.org/10.1002/2015WR017016

Chandra, S., Auken, E., Maurya, P. K., Ahmed, S., & Verma, S. K. (2019). Large Scale Mapping of Fractures and Groundwater Pathways in Crystalline Hardrock By AEM. *Scientific Reports, 9*(1), 398. https://doi.org/10.1038/s41598-018-36153-1

Chauvin, A., Gillot, P.-Y., & Bonhommet, N. (1991). Paleointensity of the Earth's magnetic field recorded by two Late Quaternary volcanic sequences at the Island of La Réunion

(Indian Ocean). *Journal of Geophysical Research: Solid Earth*, *96*(B2), 1981–2006. https://doi.org/10.1029/90JB02223

Custodio, E. (2004). Hydrogeology of volcanic rocks. In V. S. Kovalevsky, G. P. Kruseman, & K. R. Rushton, *Groundwater studies: An international guide for hydrogeological investigations* (UNESCO, Vol. 3, pp. 395–425).

Custodio, E., Garcia, L. L., & Amigo, E. (1988). Simulation par modèle mathématique de l'île volcanique de Ténériffe (Canaries, Espagne). *Hydrogéologie*, *2*(1988), 153–167.

Foged, N., Marker, P. A., Christansen, A. V., Bauer-Gottwein, P., Jørgensen, F., Høyer, A.-S., & Auken, E. (2014). Large scale 3-D modeling by integration of resistivity models and borehole data through inversion. *Hydrology and Earth System Sciences Discussions*, *11*, 1461–1492. https://doi.org/10.5194/hessd-11-1461-2014

Gailler, L.-S., & Lénat, J.-F. (2012). Internal architecture of La Réunion (Indian Ocean) inferred from geophysical data. *Journal of Volcanology and Geothermal Research*, *221–222*, 83–98. https://doi.org/10.1016/j.jvolgeores.2012.01.015

Gayer, E., Michon, L., Louvat, P., & Gaillardet, J. (2019). Storm-induced precipitation variability control of long-term erosion. *Earth and Planetary Science Letters*, *517*, 61–70. https://doi.org/10.1016/j.epsl.2019.04.003

Gingerich, S. B., & Voss, C. I. (2005). Three-dimensional variable-density flow simulation of a coastal aquifer in southern Oahu, Hawaii, USA. *Hydrogeology Journal*, *13*(2), 436–450. https://doi.org/10.1007/s10040-004-0371-z

Herrera, C., & Custodio, E. (2014). Groundwater flow in a relatively old oceanic volcanic island: The Betancuria area, Fuerteventura Island, Canary Islands, Spain. *Science of The Total Environment*, *496*, 531–550. https://doi.org/10.1016/j.scitotenv.2014.07.063

Izquierdo, T. (2014). Conceptual hydrogeological model and aquifer system classification of a small volcanic island (La Gomera; Canary Islands). *CATENA*, *114*, 119–128. https://doi.org/10.1016/j.catena.2013.11.006

Join, J. L., Folio, J. L., & Robineau, B. (2005). Aquifers and groundwater within active shield volcanoes. Evolution of conceptual models in the Piton de la Fournaise volcano. *Journal of Volcanology and Geothermal Research*, *147*(1–2), 187–201. https://doi.org/10.1016/j.jvolgeores.2005.03.013

Join, J.-L., Folio, J.-L., Bourhane, A., & Comte, J.-C. (2016). Groundwater Resources on Active Basaltic Volcanoes: Conceptual Models from La Réunion Island and Grande Comore. In P. Bachelery, J.-F. Lenat, A. D. Muro, & L. Michon (Eds.), *Active Volcanoes of the Southwest Indian Ocean* (pp. 61–70). Springer Berlin Heidelberg. https://doi.org/10.1007/978-3-642-31395-0_5

Lachassagne, P., Aunay, B., Frissant, N., Guilbert, M., & Malard, A. (2014). High-resolution conceptual hydrogeological model of complex basaltic volcanic islands: A Mayotte, Comoros, case study. *Terra Nova*, *26*(4), 307–321. https://doi.org/10.1111/ter.12102

Lénat, J. F., Gibert-Malengreau, B., & Galdéano, A. (2001). A new model for the evolution of the volcanic island of Réunion (Indian Ocean). *Journal of Geophysical Research: Solid Earth*, *106*(B5), 8645–8663. https://doi.org/10.1029/2000JB900448

411 Ley-Cooper, A. Y., Brodie, R. C., & Richardson, M. (2019). AusAEM: Australia's airborne
412 electromagnetic continental-scale acquisition program. *Exploration Geophysics*, *0*(0), 1–
413 10. https://doi.org/10.1080/08123985.2019.1694393

414 Martelet, G., Reninger, P. A., Perrin, J., & Deparis, J. (2014). *Acquisition géophysique héliportée*
415 *de l'île de La Réunion* [Report]. BRGM.

416 Minsley, B. J., Abraham, J. D., Smith, B. D., Cannia, J. C., Voss, C. I., Jorgenson, M. T.,
417 Walvoord, M. A., Wylie, B. K., Anderson, L., Ball, L. B., Deszcz-Pan, M., Wellman, T.
418 P., & Ager, T. A. (2012). Airborne electromagnetic imaging of discontinuous permafrost.
419 *Geophysical Research Letters*, *39*(2). https://doi.org/10.1029/2011GL050079

420 Oki, D. S., Souza, W. R., Bolke, E. L., & Bauer, G. R. (1998). Numerical analysis of the
421 hydrogeologic controls in a layered coastal aquifer system, Oahu, Hawaii, USA.
422 *Hydrogeology Journal*, *6*(2), 243–263. https://doi.org/10.1007/s100400050149

423 Parsekian, A. D., Singha, K., Minsley, B. J., Holbrook, W. S., & Slater, L. (2015). Multiscale
424 geophysical imaging of the critical zone. *Reviews of Geophysics*, *53*(1), 1–26.
425 https://doi.org/10.1002/2014RG000465

426 Peterson, F. L. (1972). Water development on tropical volcanic islands, type example: Hawaii.
427 *Ground Water*, *10*(5), 18–23.

428 Pryet, A., d'Ozouville, N., Violette, S., Deffontaines, B., & Auken, E. (2012). Hydrogeological
429 settings of a volcanic island (San Cristobal, Galapagos) from joint interpretation of
430 airborne electromagnetics and geomorphological observations. *Hydrology and Earth*
431 *System Sciences*, *16*(12), 4571–4579. https://doi.org/10.5194/hess-16-4571-2012

Reninger, P.-A., Martelet, G., Perrin, J., & Dumont, M. (2019). Processing methodology for regional AEM surveys and local implications. *Exploration Geophysics*. https://doi.org/10.1080/08123985.2019.1680249

Salvany, T., Lahitte, P., Nativel, P., & Gillot, P. Y. (2012). Geomorphic evolution of the Piton des Neiges volcano (Réunion Island, Indian Ocean): Competition between volcanic construction and erosion since 1.4 Ma. *Geomorphology*, *136*(1), 132–147. https://doi.org/10.1016/j.geomorph.2011.06.009

Sørensen, K. I., & Auken, E. (2004). SkyTEM ? A new high-resolution helicopter transient electromagnetic system. *Exploration Geophysics*, *35*(3), 194–202. https://doi.org/10.1071/EG04194

Viezzoli, A., Munday, T., & Cooper, Y. L. (2012). Airborne electromagnetics for groundwater salinity mapping: Case studies of coastal and inland salinisation from around the world. *Bollettino Di Geofisica Teorica Ed Applicat*, *53*(4), 581–599. https://doi.org/10.4430/bgta0067

Viezzoli, Andrea, Christiansen, A. V., Auken, E., & Sørensen, K. (2008). Quasi-3D modeling of airborne TEM data by spatially constrained inversion. *Geophysics*, *73*(3), F105–F113. https://doi.org/10.1190/1.2895521

Vittecoq, B., Deparis, J., Violette, S., Jaouën, T., & Lacquement, F. (2014). Influence of successive phases of volcanic construction and erosion on Mayotte Island's hydrogeological functioning as determined from a helicopter-borne resistivity survey correlated with borehole geological and permeability data. *Journal of Hydrology*, *509*, 519–538. https://doi.org/10.1016/j.jhydrol.2013.11.062

454 Vittecoq, B., Reninger, P.-A., Lacquement, F., Martelet, G., & Violette, S. (2019).
455 Hydrogeological conceptual model of andesitic watersheds revealed by high-resolution
456 heliborne geophysics. *Hydrology and Earth System Sciences*, *23*(5), 2321–2338.
457 https://doi.org/10.5194/hess-23-2321-2019

458 Waxman, M. H., & Smits, L. J. M. (1968). Electrical Conductivities in Oil-Bearing Shaly Sands.
459 *Society of Petroleum Engineers Journal*, *8*(02), 107–122. https://doi.org/10.2118/1863-A

460

Figure 1.

345000

350000

355000

7685000

7680000

PdN

Study area

PdF

GSAM

POE

WGS 84 / UTM 40S - EPSG : 32740

Streams

Watersheds

Springs

Salazie-Amont tunnel

GSAM

Dry portion

Water inflows

Geological map

Old basaltic lava flows (PN1 PN2)

Recent differenciated formations (PN3 PN4)

Recent pyroclastic deposits (PN4)

Figure 2.

a

RTP (nT)

2000
1000
0
-1000
-2000

0 2000 4000 6000 8000 10000

West

East

E

A

B

D

D

C

E

C

Altitude (m NGR)

1200
1000
800
600
400
200

1500
1000
500
250
100
50
Ω.m

0 2000 4000 6000 8000 10000

Distance (m)

b

c

East

Shallow aquifers

Buried valleys

Substratum

Springs

Groundwater drain

Weathering profiles

Geophysical DOI

West

Figure 3.

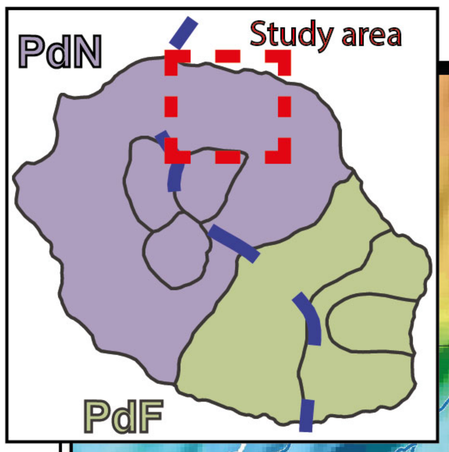

345000

350000

355000

7680000

A

B

C

D

D

GSAM

POE

2060
1380
994
740
553
409
278
162
57
-39
-128
-216
-310
-413
-527
-654
-824
-1090
-1668

RTP
[nT]

WGS 84 / UTM 40S - EPSG : 32740

Figure 4.

320000
340000
360000
7680000
7660000
7640000
1
2
3
4
5
6
7
Springs
PdN
Study area
PdF
2060
1380
994
740
553
409
278
162
57
-39
-128
-216
-310
-413
-527
-654
-824
-1090
-1668
RTP
[nT]
WGS 84 / UTM 40S - EPSG : 32740